A ES
ISSN: 2096-3246
Volume 54, Issue 02, December, 2022
Special Issue

SYNTHESES, SPECTRAL, CHARACTERIZATION AND BIOLOGICAL EVALUATION OF NEW AMINOGUANIDINE SALTS AND COPPER(II) COMPLEXES OF EDTA AND CDTA

K. Naresh
Dhanalakshmi Srinivasan College of Engineering, Coimbatore, Tamil Nadu, INDIA

Rex Jeya Rajkumar Sam david Thanapaul
Government Arts College, Udhagamandalam, The Nilgiris, India

B. N. Sivasankar*
Department of Surgery, Boston University School of Medicine, Boston, Massachusetts, USA.
sivabickol@yahoo.com

Deepika Singh
Babu Banarasi Das University, Lucknow (U.P.) India

Sneh Lata
SGT University, Gurgaon (Haryana) India

Abstract

Aminoguanidine (Agun) in aqueous solution neutralizes H_4edta (ethylenediaminetetraacetic acid) and H_4cdta (cyclohexanediaminetetraacetic acid) and replaces two acidic protons with lower pKa values to yield new salts such as diaminoguanidinium dihydrogenethylenediaminetetraacetate trihydrate, $(Agun)_2H_2edta.3H_2O$ **(L1)** and diaminoguanidiniumdihydrogencyclohexanediaminetetraacetate, $(Agun)_2H_2cdta.H_2O$ **(L2)** respectively. Two new copper(II) complexes, $(Agun)[Cu(Hedta)].3H_2O$ **(C1)** and $(Agun)[Cu(Hcdta)].H_2O$ **(C2)** have been prepared using the above ligands by the aqueous reaction between the respective ligand and copper(II) nitrate tetrahydrate in 2:1 ratio. The composition of the salts and complexes wasdone by using the basis of hydrazine, analytical and spectral techniques such as elemental analyses, IR, UV-Visible, TG-DTA, in which conformed their formation. Single crystals of **(L1), (C1)** and **(C2)** were isolated and their structures were determined by X-ray crystallography. The structure of compound **L1** reveals that this salt exists as a zwitterion in solid-state. The structural data of **C1**and **C2**shows some interesting features. Aminoguanidinium cation acts as a charge neutralizing species which is quite expected due to the steric reasons and hence could not be accommodated in the primary coordination sphere. Water molecules and aminoguanidine ion are involved in hydrogen bonding interactions and present in the secondary coordination sphere. The compound strongly bound to CT-DNA (Calf-Thymus DNA) through intercalation. The complexes have shown significant growth inhibitory activity against selected types of bacteria namely *S. pneumoniae, S. aureus, A. baumannii, P. aeruginosa, K. pneumonia,* and five fungi namely *C. albicans, C. tropicalis, T. rubrum, A. niger, A. fumigatus*. Tests on cell proliferation of human breast cancer cell lines (MCF-7), human lung cancer lines (A-549) and human cervical cell lines (HeLa)

were performed for all the compounds. The new water-soluble complexes overcome cisplatin resistance in the MCF-7, A-549, and HeLa cell lines. All the compounds were found to be non-toxic against human normal keratinocyte cells (HaCaT). The biological studies indicated that the complex **C4** exhibited better activity among the compounds and the complexes exhibited biological activity in the following order **C2>C1>L2>L1.**

Keywords:
Copper(II) complexes, Zwitterions, CT-DNA binding, Antimicrobial activity, anti-cancer studies.

Introduction

Ethylenediaminetetraacetic acid (H_4edta), cyclohexanediaminetetraacetic acid (H_4cdta) are two well known polydentate diaminopolycarboxylic acids which form a variety of coordination compounds with the metal ion in various oxidation states such as (+2, +3 and +4) states. Such complexes are water-soluble and highly stable due to the formation of ring structures. During coordination, edta and cdta ions serve as bidentate, tridentate, tetradentate, pentadentate, hexadentate or heptadentate ligand [1-5]. Hydrazine based metal-edta complexes of transition metal ions have been studied for the past few years due to their interesting structure and thermal reactivity. However, similar cdta complexes have not yet been reported in the literature [6]. Though sodium and potassium metal-edta complexes are known, the structures of these complexes resemble simple metal-edta system. However, hydrazinium ($N_2H_5^+$) metal complexes are of sufficient interest because of the coordinating ability of $N_2H_5^+$ ion and interesting thermal reactivity due to the presence of exothermic N-N bond in $N_2H_5^+$ ion. The structure and reactivity of such complexes have been studied in detail. However, similar complexes with aminoguanidinium cation, $[NH_2NHC(=NH_2)NH_2]^+$ have not been studied. This ligand has several donor atoms to compete with edta and cdta during coordination. However, this ligand is bulkier than hydrazinium cation. Hence one would expect steric factor which may not favor the inclusion of this cation in the coordination sphere. This may lead to totally unexpected structures for these aminoguanidinium metal-edta complexes.

Furthermore, the simple ligands of aminoguanidine with edta and cdta have not been reported in the literature though their hydrazinium salts were thoroughly studied. Among the metal ions in the first-row transition elements, Cu^{2+} ion is reluctant to form hydrazinium complexes due to its ease of reduction to Cu^{1+} ion and subsequently to Cu^0 in the presence of basic ligands. However, only two complexes of Cu^{2+} ions, such as hydrazinium copper oxalate [7] and hydrazinium copper ethylenediaminetetraacetate hydrate [8] have been isolated and their structure was determined. In the latter complex hydrazinium ion present inside the coordination sphere and the $Hedta^{3-}$ acts as a pentadentate ligand.

Attempts were made to prepare biologically active hydrazinium based copper carboxylates and despite many attempts, we were able to isolate only two new complexes such as two aminoguanidinium copper(II)hydrogenethylenediaminetetraacetate trihydrate and aminoguanidinium copper(II)hydrogencyclohexanediaminetetraacetate monohydrate as single crystals. It is worth to mention that the latter complex is the first metal-cyclohexanediaminetetraacetate complex with hydrazine based ligand. Hence, in this paper, we wish to report the syntheses and structures of two new copper complexes and their thermal reactivities. We also report here the preparation and characterization of aminoguanidinium salts of edta and cdta which were used as ligands in the synthesis of copper complexes and their biological properties such

as DNA/Protein binding ability, antifungal, antibacterial and anticancer activity were evaluated.

Experimental section

Materials and methods

All the chemicals used were of AnalaR or equivalent grade. The chemicals were used as received from S.D. Fine chemicals. The hydrazine contents were determined volumetrically using the KIO_3 solution (0.025 M) under Andrews's condition. The metal contents of the complexes were determined by EDTA complexometric titration [9, 10]. The C, H, and N analyses were carried out using a Perkin-Elmer (model 1240) CHN elemental analyzer.

UV-visible absorbance spectra were recorded in the range 800-200 nm using Systronics double beam 2022 spectrophotometer. IR spectra were recorded in the range of 4000-400 cm^{-1} using the Perkin-Elmer 597 spectrophotometer as KBr pellets. The simultaneous TG-DTA analyses were recorded on a SWITG/DTA 6200 thermal analyzer using 5 mg of the sample. The heating rate employed was 10 °C min^{-1} and aluminium cups were used as sample holders.

Synthesis of salts and complexes

Preparation of $(HAgun)_2H_2edta.3H_2O$ (L1)

The diaminoguanidinium dihydrogenethylenediaminetetraacetate trihydrate was prepared by adding an aqueous solution (50 mL) of aminoguanidine bicarbonate (2.72 g, 0.02 mol) to an aqueous suspension (50 mL) of H_4edta (2.92 g, 0.01 mol) with constant stirring. The resulting solution was filtered through a Whatman filter paper and the clear solution obtained was concentrated on a water bath to one-third of its original volume and kept aside at room temperature for crystallization. The colorless crystals formed after 2-3 days were removed, washed with ice-cold waterand dried in air. The crystals were further purified by recrystallization in distilled water.

$$H_4edta + 2CH_6N_4.HCO_3 \xrightarrow{H_2O} (CH_7N_4)_2H_2edta.3H_2O$$

Preparation of $(HAgun)_2H_2cdta.H_2O$ (L2)

The diaminoguanidiniumdihydrogencyclohexanediaminetetraacetate monohydrate was prepared by the neutralization reaction between H_4cdta and aminoguanidine bicarbonate. The aqueous solution (50 mL) of aminoguanidine bicarbonate (2.72 g, 0.02 mol) was added to an aqueous suspension (50 mL) of H_4cdta (3.64 g 0.01 mol) with constant stirring. The resulting solution was heated on a water bath for about 45 minutes for completion of the reaction and then the resulting solution was filtered through a Whatman filter paper. The clear solution thus obtained was concentrated on a water bath to about 50 mL and then allowed to crystallize at room temperature. The colorless crystals obtained after 48 hrs were filtered, washed with ice-cold water and dried in air.

$$H_4cdta + 2CH_6N_4.HCO_3 \xrightarrow{H_2O} (CH_7N_4)_2H_2cdta.H_2O$$

Preparation of $(HAgun)[Cu(Hedta)].3H_2O$ (C1)

Copper nitrate trihydrate (2.42 g, 0.01 mol) was dissolved in 30 ml of distilled water. To this solution, an aqueous solution of ligand, diaminoguanidinium dihydrogenethylenediaminetetraacetate trihydrate (9.9 g, 0.02 mol) in 30 mL distilled water was added with stirring. The resultant solution was kept at room temperature for 2 hours. The ethylenediaminetetraacetic acid precipitated was filtered using Whatman filterpaper and the clear solution was concentrated to 30 ml. The

concentrated solution was allowed to stand at room temperature yieldedblue crystals of the complex after 3 days which were filtered, washed quickly several times with ice-cold distilled water, and dried in air.

$$Cu(NO_3)_2.3H_2O + 2(CH_7N_4)_2H_2edta.3H_2O \xrightarrow{H_2O} (CH_7N_4)[Cu(Hedta)].3H_2O + 2CH_7N_4NO_3 + H_4edta + CH_6N_4 + 4H_2O$$

Preparation of (HAgun)[Cu(Hcdta)].H₂O (C2)

To an aqueous solution of copper nitrate trihydrate (2.42 g, 0.01 mol) in 30 mL of water, an aqueous solution (30 mL) of ligand, diaminoguanidinium dihydrogencyclohexanediaminetetraacetate monohydrate (10.23 g, 0.02 mol) was added with constant stirring. The resultant solution was kept at room temperature for 2 hours. The precipitated cyclohexanediaminetetraacetic acid was filtered and the clear solution was concentrated to 30 ml. The concentrated solution allowed standing at room temperature for crystallization. Blue crystals formed after 2-3 days were filtered, washed several times with ice-cold distilled water, and dried in air.

$$Cu(NO_3)_2.3H_2O + 2(CH_7N_4)_2H_2cdta.H_2O \xrightarrow{H_2O} (CH_7N_4)[Cu(Hcdta)].H_2O + 2CH_7N_4NO_3 + H_4cdta + CH_6N_4{+}H_2O$$

X-ray crystallography data collection and processing

X-ray single-crystal data for the complexes and the ligands were collected using the Enrus-Nonius CAD-4 diffractometer with Mo-K_α radiation (λ=0.71073A) and graphite as a monochromator. The structures were solved by the Patterson method and refined by applying full-matrix least square techniques. Refinements were carried out using the SHELEX-97 program [11, 12].Atomic scattering factors and anomalous dispersion collections were obtained from international tables for X-ray crystallography [13].The structure model was drawn using the ORTEP diagram.

DNA binding studies

Electronic absorption titration

The CT-DNA binding studies were carried out in deionized water with Tris(hydroxy-methyl)aminomethane (Tris, 5 mM) and 50 mM of NaCl adjusted to pH 7.2 with hydrochloric acid at room temperature. The concentration of CT-DNA was determined by UV absorbance at 260 nm. The solution of CT-DNA in Tris-HCl buffer gave a ratio of UV absorbance at 260 and 280 nm, A260/A280, of approximately 1.9, indicating that the DNA was sufficiently free of protein [14]. The molar absorption coefficient, ε_{260}, was taken as 6600 M^{-1} cm^{-1} [15]. Various concentrations of CT-DNA (2-2.5 μM) were added to the complexes (25 μM dissolved in DMSO/Tris-HCl buffer, 1 % DMSO in the final solution). While measuring the absorption spectra, an equal amount of DNA was added to both the test solution and the reference solution to eliminate the absorbance of DNA itself. Control experiments with DMSO were performed and no changes in the spectra of CT-DNA were observed. Absorption spectra were recorded after equilibrium at 20º C for 10 min. the intrinsic binding constant Kb was determined by using the following equation (1),

$$[DNA]/(\varepsilon_a - \varepsilon_f) = [DNA]/(\varepsilon_b - \varepsilon_f) + 1/K_b(\varepsilon_b - \varepsilon_f) \quad (1)$$

The absorption coefficients ε_a, ε_f and ε_b correspond to A_{obs}/[DNA], the extinction coefficient for the free compound, and the extinction coefficient for the compound in the fully bound form respectively. The intrinsic binding constant$K_b$can be obtained from the ratio of the slope to the intercept from the

plot of [DNA]/($\varepsilon_a - \varepsilon_f$) versus [DNA] [16].

*In vitro***antimicrobial assay**

The antimicrobial activity of the ligands (H_2L)(L1–L6)*and newly synthesized Cu(II) complexes**(C1-C6)** were evaluatedby the agar well diffusion method [17]. The test organisms, whichincluded two Gram-positive bacteria (Streptococcus pneumoniae* and *Staphylococcus aureus,* three gram-negative bacteria, *Acinetobacter baumannii, Pseudomonas aeruginosa,*and *Klebsiella pneumoniae* and five fungi *Candida albicans, Candida tropicalis, Trichophyton rubrum, Aspergillus niger, and Aspergillus fumigatus). The required nutrient broth andpotato dextrose broth were prepared and sterilized at 121 ºC. Thebacteria were grown in the nutrient broth and fungus weregrown in the potato dextrose broth at 37 ºC and maintainedon slants at 4 ºC. For all the bacterial strains, overnight culturesgrown in broth were adjusted to an inoculum size of 106 CFU permL for inoculation of the agar plates. The antimicrobial activityof the test compounds was checked with various concentrations(25 μg/mL, 50 μg/mL, and 100 μg/mL) against all the testpathogens. Gentamicin and Ketoconazole were used as positivecontrols for the antibacterial and antifungal activities, respectively. Following an incubation period of 24 h at 37 ºC, the antimicrobial activity was evaluated by the zone of inhibition. DMSOwas used both as a solvent and negative control, and no zone ofinhibition was observed for the negative control (i.e. DMSO).Each experiment was performed in triplicate and the resultswere represented as an average zone of inhibition and minimuminhibitory concentration of all the test pathogens.*

Cell cytotoxicity assay

The effects of the compounds on the viability of human breast cancer cells (MCF-7), human lung cancer cells (A549), human cervical cancer cells (HeLa) and human normal keratinocytes (HaCaT) were assayed by the3-(4, 5-dimethylthiazol-2-yl)-2,5 diphenyltetrazoliumbromide (MTT) assay [18]. The quantity of formazan formed gave a measure of the number of viable cells. The cells were seeded at a density of 10 000 cells per well in 200 mL of Dulbecco's Modified Eagle's Medium (DMEM) and were allowed to attach overnight in a CO_2 incubator, and then the complexes dissolved in DMSO were added and diluted in cell culture media to a final concentration. After 48 h, the wells were treated with 20 mL MTT (5 μg/mL PBS (phosphate-buffered saline)) and incubated at 37 ºC for 4 h. The purple formazan crystals that formed were dissolved in 200 mL of DMSO and read at 570 nm in a microplate reader. Data were obtained as the average of three independent sets of experiments all performed in triplicate for each concentration and the medium containing no test compound served as the control. The graph was plotted between the percentage of cell viability and the concentration of the compounds. The IC_{50} values were calculated from the percentage of cell viability versus concentration. The IC_{50} values of the compounds were determined by a nonlinear regression analysis using the Graph Pad Prism 5.1 [19].

Results and discussion:

The ligands were prepared by the neutralization reaction between aminoguanidine bicarbonate and H_4edta/H_4cdta in an aqueous medium. The aqueous reaction between aminoguanidinium salt of ethylenediaminetetraacetic acid/ trans-1, 2-cyclohexanediaminetetraacetic acid,and copper nitrate trihydrate yielded blue crystals ofrespective copper complexes. Both the

complexes are stable, water-soluble, and insoluble in organic solvents such as alcohol and ether. The metal and elemental analyses are following the assigned composition

1. **Diaminoguanidinium dihydrogenethylenediaminetetraacetate trihydrate (L1)**

Yield= 65 %. M. P.: 292 ºC. Molecular weight: 494.49 g/mole. Anal. Calcd for $C_{12}H_{34}N_{10}O_{11}$: N_2H_4, 12.94: C, 29.15: H, 6.93: N, 28.33 %. Found: N_2H_4, 12.58: C, 28.43: H, 6.57: N, 29.11%. IR (KBr disks, cm^{-1}): 3180 and 3500 (N-H and O-H str), 1620 (υ C=O asy), 1385 (υ C=O sym), 1120 (N-N str). UV-Vis (H_2O), λ_{max} (ε): 221 (45,126 cm) (π→π* transition), 290 (34,482 cm) (n→π* transition).

2. **Diaminoguanidinium dihydogentrans-1, 2-cyclohexanediaminetetraacetate monohydrate (L2)**

Yield= 48 %. M. P.: 320 ºC. Molecular weight: 511.35 g/mole. Anal. Calcd for $C_{16}H_{36}N_{10}O_9$: N_2H_4, 12.51: C, 35.20: H, 5.91: N, 16.42 %. Found: N_2H_4, 11.67: C, 40.86: H, 6.54: N, 20.34%. IR (KBr disks, cm^{-1}): 3200 and 3530 (N-H and O-H str), 1617 (υ C=O asy), 1417 (υ C=O sym), 1110 (N-N str). UV-Vis (H_2O), λ_{max} (ε): 218 (cm) (π→π* transition), 310 (34,482 cm) (n→π* transition).

3. **Aminoguanidinium copper(II) hydrogenethylenediaminetatraacetate trihydrate (C1)**

Yield= 70 %. M. P.: 260 ºC. Molecular weight: 481.92 g/mole. Anal. Calcd for $C_{11}H_{26}CuN_6O_{11}$: N_2H_4, 6.92: Cu, 13.19: C, 27.41: H, 5.43: N, 17.44 %. Found: N_2H_4, 7.21: Cu, 12.96: C, 26.93: H, 5.27: N, 16.98 %. IR (KBr disks, cm^{-1}): 3180 and 3400 (N-H and O-H str), 1610 (υ C=O asy), 1394 (υ C=O sym), 1726 (COOH), 1099 (N-N str). UV-Vis (H_2O), λ_{max} (ε): 240 (cm) (π→π* transition), 345 (34,482 cm) (n→π* transition), 740 (cm) (d-d transition).

4. **Aminoguanidinium copper(II) hydrogentrans-1, 2-cyclohexanetetraacetate monohydrate (C2)**

Yield= 68 %. M. P.: 292 ºC. Molecular weight: 499.97 g/mole. Anal. Calcd for $C_{15}H_{28}CuN_6O_9$: N_2H_4, 7.11: Cu, 12.71: C, 36.03: H, 5.64: N, 16.81 %. Found: N_2H_4, 9.45: Cu, 12.37: C, 26.93: H, 5.74: N, 16.48 %. IR (KBr disks, cm^{-1}): 3450 and 3200 (N-H and O-H str), 1620 (υ C=O asy), 1380 (υ C=O sym), 1727 (COOH), 1105 (N-N str). UV-Vis (H_2O), λ_{max} (ε): 240 (cm) (π→π* transition), 330 (34,482 cm) (n→π* transition), 695 (cm) (d-d transition).

Electronic spectra

The electronic spectrum of **C1**(Fig. 1) shows a band at 695 nm for the transition from B_1 state to A_1, B_2 and Eexcited states. In this stage, the square pyramidal geometry could be proposed for the complex. However, for the octahedral Cu(II) environment broadband is expected around 740 nm (13,510 cm). The other bands observed in the higher energy region (345 and 235 nm) are attributed to the intra-ligand transition. However, the X-ray structure reveals octahedral geometry, and one Cu-O bond is found to be very weak.

The electronic spectrum of **C2**(Fig. 2) displays a lower energy band at 695 nm (14,390 cm), which corresponds to the transition from the $B_1(d_{x^2-y^2})$ ground states to the excited $A_1(d_{z^2})$, $B_2(d_{xy})$ and $E(d_{xz}, d_{yz})$ states. This d-d transition indicates that the copper has a square pyramidal geometry [20]. Higher energy-intense transitions at 330 and 240 nm are assigned to intraligand $\pi\rightarrow\pi^*$ and $n\rightarrow\pi^*$ charge transfer transitions (ILCT- intraligand charge transfer transition), respectively.In contrast, trigonal bipyramidal Cu(II) complexes usually show a maximum at >800 nm (d_{xy}, $d_{x^2-y^2}\rightarrow d_{z^2}$) with a higher energy shoulder (spin allowedd_{xz}, $d_{yz}\rightarrow d_{z^2}$).

Infrared spectra

The IR spectra of both the ligands show broad bands in the region 3180-3500 cm^{-1} with splitting which is quite expected and assigned for the stretching vibrations of different types of N-H bonds such as C-N-H, present in the aminoguanidinium ion and the H_2edta^{2-} or H_2cdta^{2-}zwitterion. Besides these, N-H and O-H stretchings of water molecules and free carboxylic acid groups also the reason for the splitting. Two types of carbonyl stretchings are expected for free carboxylic acid groups and carboxylate ions. However, absences of any band in the region 1720-1730 cm^{-1} indicating the absence of free carboxylic acid groups. Hence, zwitterion formation is proposed based on IR data. Two bands observed around 1620 cm^{-1} and 1385 cm^{-1} are assigned for $\nu_{asy}$and ν_{sym}stretchings of carboxylate ions respectively. The N-N stretching of aminoguanidinium cation is observed at 1120 cm^{-1} for $(HAgun)(H_2edta).3H_2O$ and 1110 cm^{-1} for $(HAgun)(H_2cdta).H_2O$. Similar aminoguanidinium salts of dicarboxylic acids such as oxalic acid and succinic acid were also reported [21] to show the N-N stretching in this region.

The IR spectrum of **C1**is shown in Fig. 3. In the spectrum, the asymmetric and symmetric stretching frequency of carboxylate ions is observed at 1610 cm^{-1} and 1394 cm^{-1} respectively. The $\Delta\nu$ separation (ν_{asy}-ν_{sym}) is 216 cm^{-1} which indicates the monodentate coordination behavior of carboxylate ions. The carbonyl stretching of the free carboxylic acid is expected above 1700 cm^{-1} and in the present case, it is seen at 1726 cm^{-1}. A sharp band at 1683 cm^{-1} and a week band at 1099 cm^{-1} are assigned to the iminidinium ($C{=}NH_2^+$) and N-N stretching vibrations respectively, which confirm the presence of aminoguanidinium cation. Several bands observed in the region 3180-3400 cm^{-1} are attributed to the N-H and O-H stretching of aminoguanidinium cation and water molecules respectively [22].

The IR spectrum of **C2** is shown in Fig. 4. This is similar to complex **C1**. Two bands observed at 1620 and 1380 cm^{-1} are assigned to ν_{asy} and ν_{sym} stretching of carboxylate ions with $\Delta\nu$= 240 cm^{-1} corresponds to their monodentate coordination. The sharp band observed at 1727 cm^{-1} is assigned to the carbonyl stretching of free carboxylic acid. The presence of aminoguanidinium cation is revealed by the C-N stretching vibration of iminidinium ion ($C{=}NH_2^+$) and N-N stretching vibration at 1672 and 1105 cm^{-1} respectively. Several weak and sharp bands observed between 3450 and 3200 $cm^{-1}$are attributed to the N-H and O-H stretching vibrations of aminoguanidinium cation and water molecules respectively [23].

The hydrazinium copper-edta monohydrate has an octahedral structure with pentadentate $Hedta^{3-}$ and one coordinated hydrazinium cation [24]. Simple copper-edta monohydrate is also octahedral with pentadentate $Hedta^{3-}$ and a coordinated water molecule. In the present case aminoguanidinium cation is not coordinated, could be due to its larger size, and the water molecule is expected to coordinate with a metal ion to complete the octahedral coordination. However, in the absence of other studies such as TG-DTA and X-ray crystallography, it is very difficult to assign the exact structures of the complexes.

Thermal degradation study

Simultaneous TG-DTA of diaminoguanidinium dihydrogenethylenediaminetetraacetate trihydrate (Fig. 5) reveals that this salt initially undergoes dehydration (73-110 °C) without melting. Further decomposition continues at higher temperatures upto 800 °C. An endotherm for the first stage is observed with the weight loss of 11.2 % in TG which is in good agreement with the calculated

value for the elimination of three water molecules. However, after dehydration, the degradation is gradual and complete decomposition is observed with 100% weight loss.

Diaminoguanidiniumdihydrogencyclohexanediaminetetraacetate monohydrate (Fig. 6) also shows similar dehydration behavior like that of edta salt. Endotherm for dehydration is weak and broad and observed between 80-100 °C. The weight loss observed is 4.10% in the rangewhich is expected for the removal of one water molecule. After dehydration, continuous degradation takes place with several weak endotherms in the DTA, leaving no residue at 800 °C. This salt also undergoes degradation without melting.

Both the complexes decompose in a similar pattern. The first stage is endothermic dehydration which is followed by the loss of aminoguanidine which is exothermic. Then the copper-H_2edta/H_2cdta intermediates formed undergo ligand pyrolysis to yield $CuCO_3$ as end residue via copper acetate. The simultaneous TG-DTA traces of **C1** and **C2** are shown in Fig. 7 and 8 respectively. The thermal degradation data of the salts and complexes are presented in Table 1.

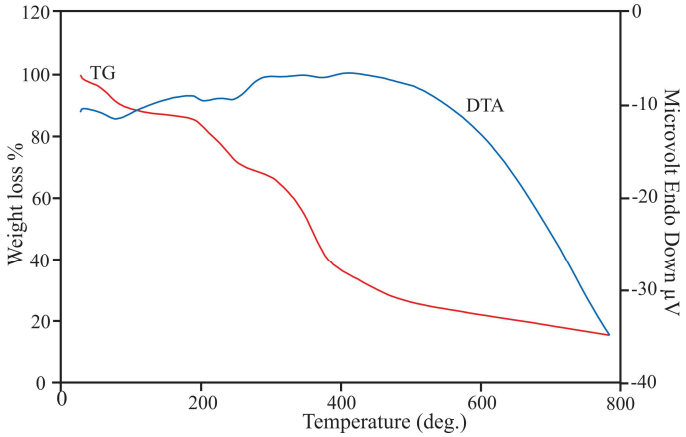

Fig. 5. Simultaneous TG-DTA of $(HAgun)_2(H_2edta).3H_2O$

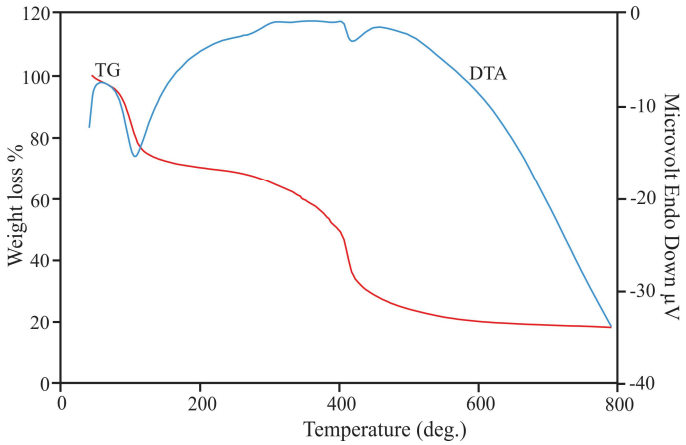

Fig. 6. Simultaneous TG-DTA of $(HAgun)_2(H_2cdta).H_2O$

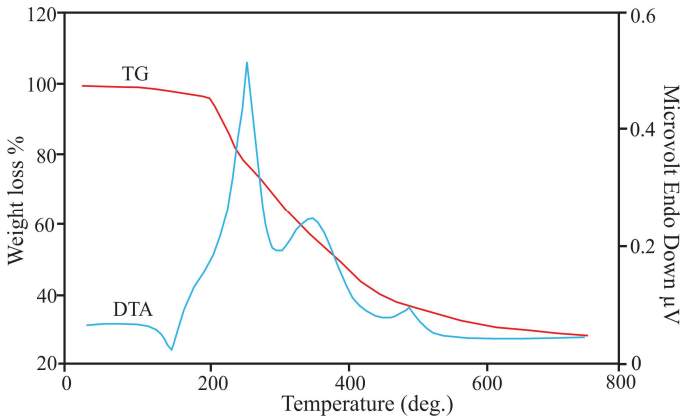

Fig. 7. Simultaneous TG-DTA of(HAgun)[Cu(Hedta)].3H_2O

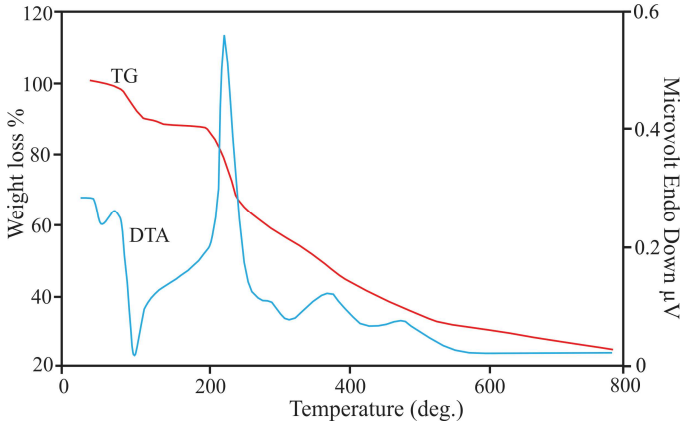

Fig. 8. Simultaneous TG-DTA of (HAgun)[Cu(Hcdta)].H_2O

Crystal structures

Crystal structures of several octahedral complexes of Cu(II) such as [Cu(H_2edta)(H_2O)], NH_4[Cu(Hedta)(H_2O)], N_2H_5[Cu(Hedta)(H_2O)], etc., have been reported in the literature [25]. In all the above cases Cu^{2+} ion was surrounded by $Hedta^{(4-n)-}$ ion and water/ hydrazinium molecule. However, complexes with polymeric structures and octahedral geometry around Cu^{2+} ion have not been reported so far. The structure and geometry of Cu(II) complexes can be modified by changing the counter ion in the place of NH_4^+ and $N_2H_5^+$ ions. By substitution or introducing ring structure in edta can also largely modify the geometry. During our investigation on hydrazine and its derivatives of metal diaminopolycarboxylate system, we have reported several hydrazinium and phenyl hydrazinium metal(II) and metal(III) ethylenediaminetetraacetate and their hydrates [26]. In all the cases it was observed that the $Hedta^{3-}$ or $edta^{4-}$ coordinated to the central metal ions as a pentadentate or hexadentate ligand and the complexes were found to be monomeric. The bridged mode was observed only in the simple lanthanide-edta complexes except in the case of recently reported Pr(III) complex [27]. Because of the hexadentate nature of $cdta^{4-}$ the steric make-up of its back bone, will not allow coordination of additional ligand and hence expected to show interesting structural features.

The ORTEP and packing diagrams of **L1** are given in Figs.9 and10 respectively. This salt crystallizes as a monoclinic system with P2/n space group. The crystal density observed from X-ray study is 1.474mg/m^3 which is very close to the experimental value (1.379 mg/m^3). The number of molecules in the unit cell is 2. The X-ray crystal data of this salt is given in Table 3 and the bond

distances, bond angles, and hydrogen bondings are given in Table 2, 3, 4, and 5 respectively. The crystal structure of this salt shows that it consists of three discrete ions such as two aminoguanidinium cations and a carboxylate anion. The anion has C_2 axis of symmetry and the axis passing through C-C bond of ethylenic carbon atoms cuts the anion into two equal half and one halves is exactly trans to the other. The tertiary nitrogen atoms of $edta^{4-}$ are protonated and hence the salt behaves as a zwitterion even in solid-state.

The ORTEP diagram of **C1** is shown in Fig. 11 along with atom labeling. The polymeric structure is given in Fig. 12 and the packing diagram is given in Fig. 13. The complex crystallized in monoclinic crystal system with $P2_1/n$ space group. The number of molecules in the unit cell is 4. The copper ion of the complex is octahedrally surrounded by two carboxyl oxygen atoms and two tertiary nitrogen atoms and one carboxyl oxygen atom of the third carboxylate group of the anion, $Hedta^{3-}$. Cu-O bond distances of two oxygen atoms was the same 1.9740 Å (15) and longer than the other Cu-O bond lengths. One carboxylate oxygen of the third carboxylate group coordinated to second copper(II) ion resulting in the bridged structure. One carboxylic acid groups are free and not involved in coordination. The bridging nature of $Hedta^{3-}$ ion in the copper complex is observed for the first time. Water molecules forming a hydrogen bond with carboxylate oxygen atom is the reason for dehydration at higher temperature though they are not coordinated to the metal ion. The bond distances and bond angles together with their estimated standard deviation derived from the least square inverse matrix and hydrogen bonding are given in Tables 2,3, 4, and 6 respectively.

The potentially hexadentate edta ligand is only acting as a quinquedntate ligand in this complex and aminoguanidinium cation is not coordinated to the Cu(II) ion which is attributed to its bulky nature.

The ORTEP diagram of **C2** is shown in Fig. 14. The packing diagram is given in Fig. 15. The crystal system is monoclinic and the space groupis$P2_1/c$.The number of molecules in the unit cell is 4. Structural analysis reveals an unexpected five coordinated environment around Cu^{2+} ion in this complex though octahedral geometry is expected with polyaminopolycarboxylicacids. Cu_1-O(4) distance of 2.237(20) Å is longer than the other two Cu_1-O(1)/O(5) bonds, 1.966(2) Å and 1.913(2) Å indicating that the coordination geometry is close to square-based pyramidal with carboxylate oxygen (O(4)) of $cdta^{3-}$ in the apical position. Cu_1-N_1 (2.029(2) Å) and Cu_1-N_2(2.030(2) Å) bond lengths are almost equal indicating similar interaction and position. One free carboxylic acid group is observed which is not coordinated to the metal ion. Bond distances, bond angles, and hydrogen bonds are given in Tables2, 3, 4, and 7 respectively.

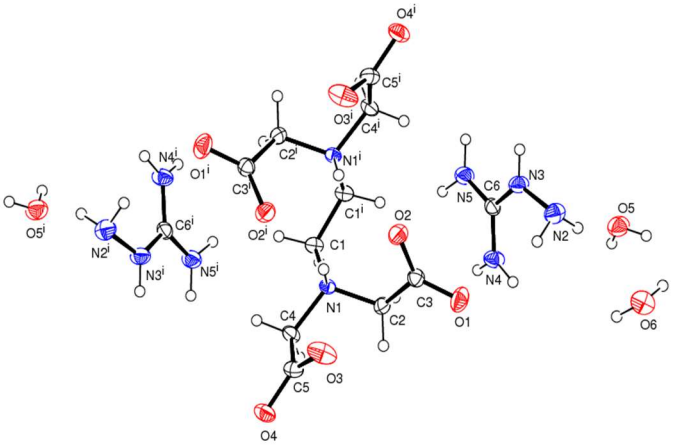

Fig. 9. ORTEP of $(HAgun)_2[H_2edta].3H_2O$

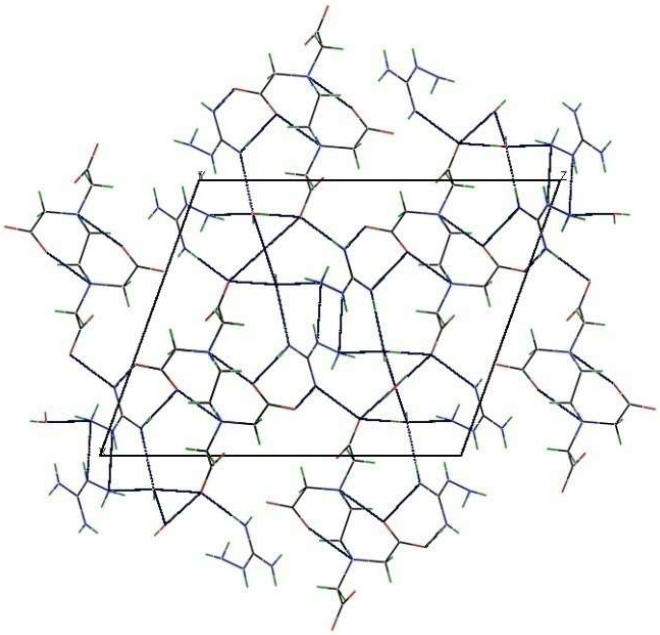

Fig. 10. Packing diagram of $(HAgun)_2[H_2edta].3H_2O$

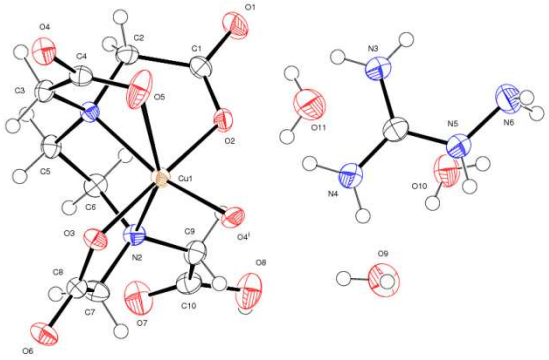

Fig. 11.ORTEP diagram of $(HAgun)[Cu(Hedta)].3H_2O$

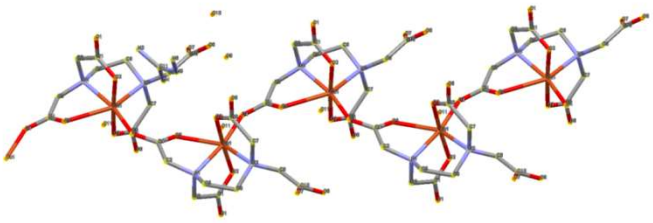

Fig. 12. Polymeric structure of (HAgun)[Cu(Hedta)].3H_2O

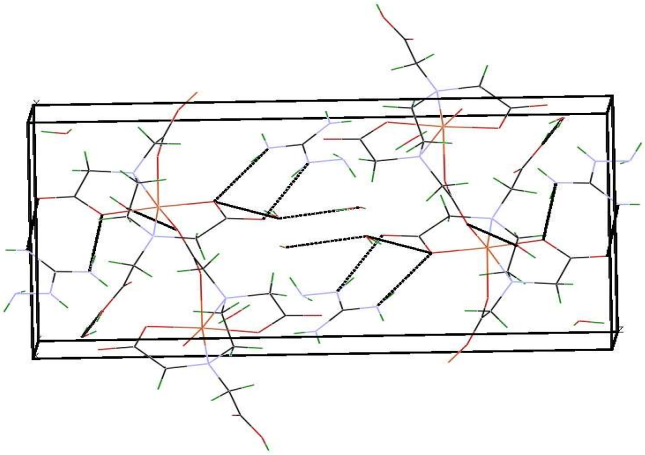

Fig. 13. Packing diagram of (HAgun)[Cu(Hedta)].3H_2O

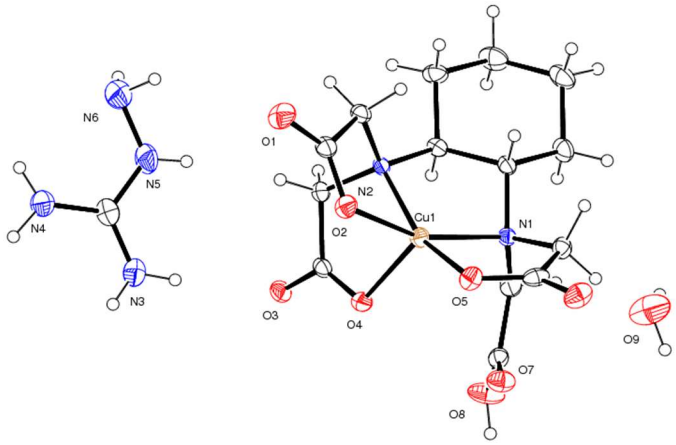

Fig. 14.ORTEP diagram of (HAgun)[Cu(Hcdta)].H_2O

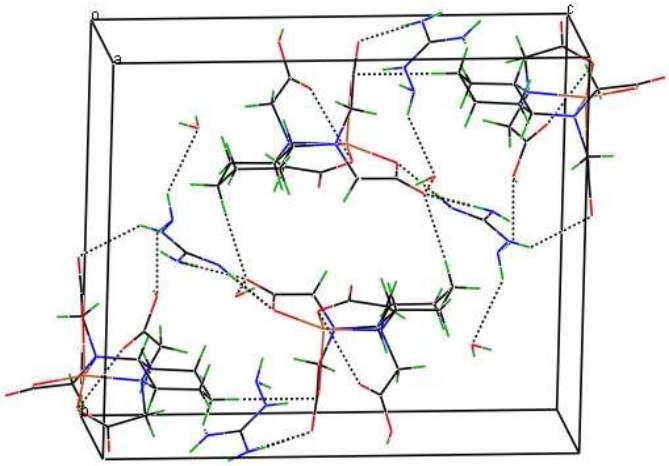

Fig. 15. Packing diagramof (HAgun)[Cu(Hcdta)].H_2O

The steric factor plays an important role in building the structure of complexes. Though six coordination is common and several donor atoms are available for occupying the sixth site of an octahedron from the aminoguanidinium ion, water molecule and carboxylic acid oxygen donor atoms, the presence of cyclohexane ring imposes a steric factor which prevents another donor site to approach the central Cu^{2+} ion. In simple $CuH_2edta.H_2O$ and $N_2H_5CuHedta.H_2O$ complexes along with the pentadentate $Hedta^{3-}$ ion six coordination was observed in the former case with coordinated water [25] and in the latter case, hydrazinium cation occupies the sixth site of an octahedron [28]. In the present case, despite the presence of few nitrogen donor atoms in the aminoguanidinium cation and oxygen donor atom in the water molecule, their coordination to the sterically hindered metal ion is less feasible. Hence aminoguanidinium cation present outside the sphere as charge neutralizing species and water molecule occupy the secondary coordination sphere as lattice water which is well supported by its endothermic dehydration at a lower temperature in TG-DTA analysis.

As expected, chelation and construction of the five-membered rings always stabilize the system. This type of chelation is unique for complexes containing aminopolycarboxylates. Due to the larger size factor, contrary to $N_2H_5^+$ cation aminoguanidinium cation is not expected to coordinate to the metal ion in the presence of strong chelating $Hedta^{3-}$ ion, and hence present as a counter ion for charge neutralization.

Table 2. Crystallographic data of the compounds **L1**, **C1**, **C2**

Compound	**L1**	**C1**	**C2**
CCDC No	1498779	1497022	1517522
Empirical formula	C_{12} H_{34} N_{10} O_{11}	C_{11} H_{26} Cu N_6 O_{11}	C_{15} H_{28} Cu N_6 O_9
Formula weight	494.49	481.92	499.97
Temperature	293 K	296 K	296 K
Wavelength	0.71073 Å	0.71073 Å	0.71073 Å
Crystal system	Monoclinic	Monoclinic	Monoclinic
Space group	P2/n	$P2_1/n$	$P2_1/c$
Unit cell dimensions	a = 13.1951 Å□□□□□= 90°.	a = 9.8675 Å □= 90°.	a = 8.7327 Å □□= 90°.
	b = 5.4834 Å □□□=	b = 10.2893 Å □=	b = 13.8293 Å□□□=

	109.944(3)°.	95.418(2)°.	97.740(3)°.
	c = 16.3819 Å □□ = 90°.	c = 18.8130 Å □ = 90°.	c = 17.0421 Å □ = 90°.
Volume	1114.21 $Å^3$	1901.54 $Å^3$	2039.4 $Å^3$
Z	2	4	4
Density (calculated)	1.474 Mg/m^3	1.683 Mg/m^3	1.628 Mg/m^3
Absorption coefficient	0.128 mm^{-1}	1.220 mm^{-1}	1.134 mm^{-1}
F(000)	528	1004	1044
Crystal size	0.300 x 0.300 x 0.250 mm^3	0.400 x 0.300 x 0.200 mm^3	0.200 x 0.150 x 0.100 mm^3
Theta range for data collection	2.645 to 24.999°.	2.175 to 24.999°.	2.354 to 26.386°.
Index ranges	-15<=h<=15, -6<=k<=6, -19<=l<=19	-11<=h<=11, -12<=k<=12, -22<=l<=22	-10<=h<=10, -17<=k<=17, -21<=l<=21
Reflections collected	11864	27202	32257
Independent reflections	1980 [R(int) = 0.0241]	3342 [R(int) = 0.0223]	4180 [R(int) = 0.0750]
Completeness to theta = 24.999°	99.90 %	100.00 %	100.00 %
Absorption correction	Semi-empirical from equivalents	Semi-empirical from equivalents	Semi-empirical from equivalents
Max. and min. transmission	0.976 and 0.957	0.81 and 0.59	0.87 and 0.75
Refinement method	Full-matrix least-squares on F^2	Full-matrix least-squares on F^2	Full-matrix least-squares on F^2
Data / restraints / parameters	1980 / 0 / 195	3342 / 13 / 315	4180 / 24 / 331
Goodness-of-fit on F2	1.03	1.076	1.074
Final R indices [I>2sigma(I)]	R1 = 0.0302, wR2 = 0.0741	R1 = 0.0271, wR2 = 0.0738	R1 = 0.0399, wR2 = 0.0968
R indices (all data)	R1 = 0.0392, wR2 = 0.0813	R1 = 0.0308, wR2 = 0.0772	R1 = 0.0731, wR2 = 0.1162
Extinction coefficient	0.0085(17)	N/A	N/A
Largest diff. peak and hole	0.182 and -0.170 $e.Å^{-3}$	0.299 and -0.408 $e.Å^{-3}$	0.996 and -0.321 $e.Å^{-3}$

Table 3. Bond lengths

L1		C1		C2	
C(1)-N(1)	1.5030(17)	C(1)-O(1)	1.222(3)	C(8)-O(1)	1.237(4)
C(2)-N(1)	1.5023(17)	C(1)-O(2)	1.276(3)	C(8)-O(2)	1.281(4)
C(3)-O(1)	1.2417(17)	C(4)-O(5)	1.218(3)	C(10)-O(4)	1.247(3)
C(3)-O(2)	1.2572(17)	C(4)-O(4)	1.273(3)	C(10)-O(3)	1.270(4)
C(4)-N(1)	1.4943(17)	C(8)-O(6)	1.237(3)	C(12)-O(6)	1.224(4)
C(4)-C(5)	1.524(2)	C(8)-O(3)	1.272(3)	C(12)-O(5)	1.287(4)
C(5)-O(3)	1.2248(18)	C(10)-O(7)	1.198(3)	C(14)-O(7)	1.195(4)
C(5)-O(4)	1.2658(17)	C(10)-O(8)	1.330(3)	C(14)-O(8)	1.322(4)
C(6)-N(4)	1.3187(19)	N(1)-Cu(1)	2.0786(17)	N(1)-Cu(1)	2.029(2)
C(6)-N(5)	1.321(2)	N(2)-Cu(1)	2.3406(18)	N(2)-Cu(1)	2.030(2)
C(6)-N(3)	1.3346(19)	N(5)-N(6)	1.395(3)	N(5)-N(6)	1.401(5)
N(2)-N(3)	1.4068(19)	O(2)-Cu(1)	1.9230(15)	O(2)-Cu(1)	1.966(2)
		O(3)-Cu(1)	1.9526(15)	O(4)-Cu(1)	2.234(2)
		O(4)-Cu(1)#1	1.9740(15)	O(5)-Cu(1)	1.913(2)
		Cu(1)-O(4)#2	1.9740(15)		

Table 4. Bond angles

L1		C1		C2	
N(1)-C(1)-C(1)#1	114.59(10)	C(3)-N(1)-Cu(1)	110.64(13)	C(13)-N(1)-Cu(1)	116.10(18)
N(1)-C(2)-C(3)	111.42(11)	C(2)-N(1)-Cu(1)	105.57(12)	C(11)-N(1)-Cu(1)	104.65(17)
O(1)-C(3)-O(2)	126.80(13)	C(5)-N(1)-Cu(1)	108.08(13)	C(1)-N(1)-Cu(1)	100.89(16)
O(1)-C(3)-C(2)	116.05(12)	C(9)-N(2)-Cu(1)	109.34(13)	C(9)-N(2)-Cu(1)	110.60(17)
O(2)-C(3)-C(2)	117.14(12)	C(7)-N(2)-Cu(1)	103.60(13)	C(7)-N(2)-Cu(1)	101.01(17)
N(1)-C(4)-C(5)	110.73(11)	C(6)-N(2)-Cu(1)	101.81(12)	C(6)-N(2)-Cu(1)	107.00(17)
O(3)-C(5)-O(4)	126.43(14)	C(11)-N(5)-N(6)	121.0(2)	C(8)-O(2)-Cu(1)	112.33(18)
O(3)-C(5)-C(4)	118.69(12)	C(1)-O(2)-Cu(1)	117.04(14)	C(10)-O(4)-Cu(1)	111.51(18)
O(4)-C(5)-C(4)	114.87(13)	C(8)-O(3)-Cu(1)	119.34(14)	C(12)-O(5)-Cu(1)	114.58(19)
N(4)-C(6)-N(5)	120.32(14)	C(4)-O(4)-Cu(1)#1	127.96(15)	O(5)-Cu(1)-O(2)	94.32(9)
N(4)-C(6)-N(3)	120.97(14)	O(2)-Cu(1)-O(3)	174.20(7)	O(5)-Cu(1)-N(1)	87.08(9)
N(5)-C(6)-N(3)	118.69(13)	O(2)-Cu(1)-O(4)#2	89.96(7)	O(2)-Cu(1)-N(1)	160.25(9)
C(4)-N(1)-C(2)	111.58(10)	O(3)-Cu(1)-O(4)#2	92.46(7)	O(5)-Cu(1)-N(2)	160.60(9)
C(4)-N(1)-C(1)	110.73(10)	O(2)-Cu(1)-N(1)	85.20(7)	O(2)-Cu(1)-N(2)	83.27(9)
C(2)-N(1)-C(1)	113.74(11)	O(3)-Cu(1)-N(1)	93.91(7)	N(1)-Cu(1)-N(2)	88.90(9)
C(6)-N(3)-N(2)	123.82(13)	O(4)#2-Cu(1)-N(1)	163.18(7)	O(5)-Cu(1)-O(4)	119.72(8)
		O(2)-Cu(1)-N(2)	93.95(7)	O(2)-Cu(1)-O(4)	101.22(9)
		O(3)-Cu(1)-N(2)	80.25(6)	N(1)-Cu(1)-O(4)	95.10(8)
		O(4)#2-Cu(1)-N(2)	113.99(7)	N(2)-Cu(1)-O(4)	79.53(8)
		N(1)-Cu(1)-N(2)	82.46(7)		

Table 5. Hydrogen bonding interaction of compound **L1** [Å and °].

D-H...A	d(D-H)	d(H...A)	d(D...A)	<(DHA)
C(1)-H(1B)...O(3)#2	0.97	2.28	3.1644(17)	150.9
C(2)-H(2B)...O(1)#3	0.97	2.61	3.5472(18)	163.6
C(4)-H(4A)...O(3)#2	0.97	2.62	3.3515(19)	132.0
N(3)-H(3A)...N(2)#4	0.852(19)	2.309(19)	3.0311(19)	142.7(16)
N(5)-H(5A)...O(2)#2	0.89(2)	2.00(2)	2.8836(18)	171.2(16)
N(2)-H(2D)...O(5)	0.91(2)	2.21(2)	3.042(2)	152.4(17)
N(4)-H(4D)...O(1)#2	0.884(19)	1.97(2)	2.8496(18)	172.6(16)
N(5)-H(5B)...O(5)#5	0.91(2)	1.90(2)	2.8021(18)	174.0(18)
N(4)-H(4C)...O(4)#3	0.90(2)	2.08(2)	2.9668(18)	170.8(18)
N(2)-H(2C)...O(1)	0.92(2)	2.50(2)	3.361(2)	156.3(17)
N(1)-H(1)...O(2)	0.908(17)	2.205(16)	2.6794(15)	111.9(12)
N(1)-H(1)...O(2)#1	0.908(17)	2.175(17)	2.8898(16)	135.1(13)
O(6)-H(6A)...O(4)#3	0.87(2)	1.82(2)	2.6914(15)	176(2)
O(5)-H(5C)...O(4)#6	0.83(3)	1.96(3)	2.7644(19)	166(2)
O(5)-H(5D)...O(6)#2	0.86(3)	1.89(3)	2.7268(19)	166(2)

Symmetry transformations used to generate equivalent atoms:
#1 -x+1/2,y,-z+3/2; #2 x,y+1,z ;#3 -x,-y+1,-z+1; #4 -x+1,-y+1,-z+; #5 -x+1,-y+2,-z+1; #6 x+1/2,-y+1,z-1/2

Table 6. Hydrogen bonding interaction of compound **C1** [Å and °].

D-H...A	d(D-H)	d(H...A)	d(D...A)	<(DHA)
C(2)-H(2A)...O(9)#3	0.97	2.55	3.522(3)	176.4
C(3)-H(3B)...O(8)#3	0.97	2.63	3.559(3)	160.7
C(5)-H(5B)...O(7)#4	0.97	2.55	3.503(3)	166.5
C(6)-H(6A)...O(7)	0.97	2.60	3.075(3)	110.2
C(6)-H(6B)...O(1)#5	0.97	2.43	3.319(3)	152.2
C(7)-H(7A)...O(11)#2	0.97	2.58	3.549(4)	176.0
C(9)-H(9A)...O(5)#2	0.97	2.31	3.162(3)	146.0
C(9)-H(9B)...O(2)	0.97	2.65	3.271(3)	122.0
O(8)-H(8)...O(10)#6	0.82	1.76	2.558(2)	163.3
O(10)-H(10B)...O(9)	0.830(18)	1.94(2)	2.748(3)	165(3)
N(3)-H(3D)...O(11)#7	0.828(18)	2.344(19)	3.162(3)	170(3)
N(4)-H(4A)...O(2)	0.871(17)	1.977(19)	2.839(3)	170(3)
N(3)-H(3C)...O(1)	0.856(17)	2.173(18)	3.029(3)	179(3)
N(6)-H(6D)...O(1)#7	0.870(18)	2.31(2)	3.107(3)	153(3)
N(4)-H(4B)...O(3)#2	0.870(17)	2.163(18)	3.028(3)	173(3)
N(5)-H(5)...O(6)#2	0.858(18)	2.06(2)	2.894(3)	164(3)
N(6)-H(6C)...O(6)#8	0.881(18)	2.17(2)	3.001(3)	158(3)
O(10)-H(10A)...O(6)#8	0.826(18)	1.90(2)	2.709(3)	167(3)
O(9)-H(9D)...O(8)	0.829(18)	2.06(2)	2.872(3)	167(3)

O(11)-H(11B)...O(4)#2	0.830(19)	2.073(19)	2.903(3)	178(4)
O(11)-H(11A)...N(6)#7	0.831(19)	2.24(3)	3.005(4)	154(4)
O(9)-H(9C)...O(3)#2	0.819(19)	2.21(2)	3.007(3)	164(4)

Symmetry transformations used to generate equivalent atoms:
#1 -x+1/2,y+1/2,-z+1/2 #2 -x+1/2,y-1/2,-z+1/2#3 x,y+1,z #4 -x-1/2,y+1/2,-z+1/2 #5 -x, y+1,-z#6 -x,-y,-z #7 -x+1,-y+1,-z #8 x+1/2,-y+1/2,z-1/2

Table 7. Hydrogen bonding interaction of compound **C2** [Å and °].

D-H...A	d(D-H)	d(H...A)	d(D...A)	<(DHA)
C(1)-H(1)...O(6)#1	0.98	2.50	3.390(4)	151.4
C(2)-H(2A)...N(6)#2	0.97	2.64	3.411(5)	136.5
C(5)-H(5B)...O(7)#3	0.97	2.58	3.525(4)	166.2
C(7)-H(7A)...O(6)#3	0.97	2.60	3.277(4)	127.3
C(7)-H(7B)...O(6)#1	0.97	2.50	3.289(4)	138.1
C(13)-H(13A)...O(9)	0.97	2.57	3.479(8)	156.4
O(8)-H(8)...O(3)#4	0.82	1.81	2.610(3)	163.9
O(9)-H(9C)...O(5)#5	0.86(2)	1.98(2)	2.837(7)	171(7)
O(9)-H(9D)...O(1)#2	0.85(2)	2.10(2)	2.951(8)	175(8)
O(9')-H(9E)...O(5)#5	0.85(2)	2.42(13)	2.769(11)	105(10)
O(9')-H(9F)...O(1)#2	0.85(2)	2.20(4)	3.033(11)	164(10)
N(3)-H(3C)...O(3)	0.82(4)	2.08(4)	2.899(4)	176(4)
N(3)-H(3D)...O(1)#6	0.89(3)	2.01(4)	2.887(4)	172(3)
N(4)-H(4C)...O(2)#6	0.88(5)	2.03(5)	2.906(4)	173(4)
N(4)-H(4D)...O(9')#7	0.88(4)	2.39(4)	3.084(16)	136(3)
N(5)-H(5)...O(3)#7	0.83(4)	2.41(4)	3.061(4)	136(4)
N(6)-H(6C)...O(9)#8	0.97(6)	2.48(6)	3.311(14)	143(5)
N(6)-H(6D)...O(4)#3	0.85(5)	2.44(5)	3.059(4)	130(4)
N(6)-H(6D)...O(8)#7	0.85(5)	2.46(5)	3.110(6)	133(4)

Symmetry transformations used to generate equivalent atoms:
#1 -x,-y,-z+2 #2 x-1,-y+1/2,z-1/2 #3 x+1,y,z#4 -x,-y+1,-z+2 #5 x,-y+1/2,z-1/2 #6 -x+1,y+1/2,-z+5/2#7 -x+1,-y+1,-z+2 #8 x+1,-y+1/2,z+1/2

DNA binding experiments

Absorption spectral titrations

The UV-Vis absorption titration spectroscopy for the greatest part used to evaluate the interaction of Calf-Thymus (CT-DNA) with copper(II) complexes **(C1-C2)** (Fig.). This absorption titration technique implicates monitoring the changes in the UV-Vis spectrum of the ligands and complexes during its interaction with Calf-Thymus (CT-DNA). The ligands and complexes with DNA interaction are determined by examining the modification in the λ_{max} values of π-π^* intra-ligand transitions, LMCT (ligand to metal charge transfer), and d-d transition of the metal complexes with the increase in the concentration of CT-DNA. The intercalative mode of binding of ligands and metal complexes to DNA was indicated by hypsochromism, bathochromism and hyperchromism, while

hyperchromism intimate electrostatic interaction or groove binding. The extent of changes in the absorption spectrum of the ligands and metal complexes are consistent with the strength of DNA interaction.

In our study, all the ligands and copper(II) complexes shows hypsochromism and bathochromism with the increase inthe concentration of DNA indicating the binding of ligands and complexes through intercalation.The binding constant values were calculated from the plot of[DNA]/(ε_a-ε_f) versus [DNA](Fig. 16 (a), (b)). The binding affinities of the ligands and complexes were quantitatively expressed in terms of intrinsic binding constant k_b which is found to follow the order for the ligands and complexes respectively,**C2 > C1.** The k_b values were determined using equation (1) given below is found to be C2 is 8.63×10^6 M^{-1} and C1 is 5.1×10^6 M^{-1}. The observed hypochromism, redshift, and binding constant values showed that all the complexes bind to DNA via an intercalative mode [29, 30]. The extend of the hypochromism commonly parallels the intercalative binding affinity. These obtained results are comparable with the DNA binding affinity of the previously reported various copper compound intercalators [31-33]

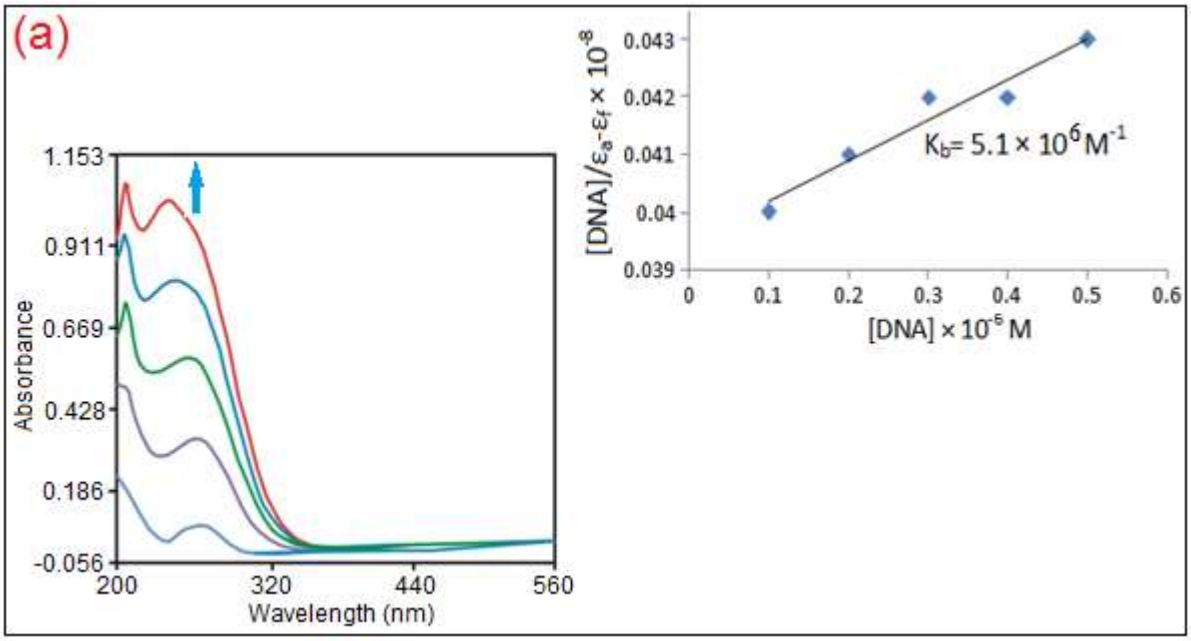

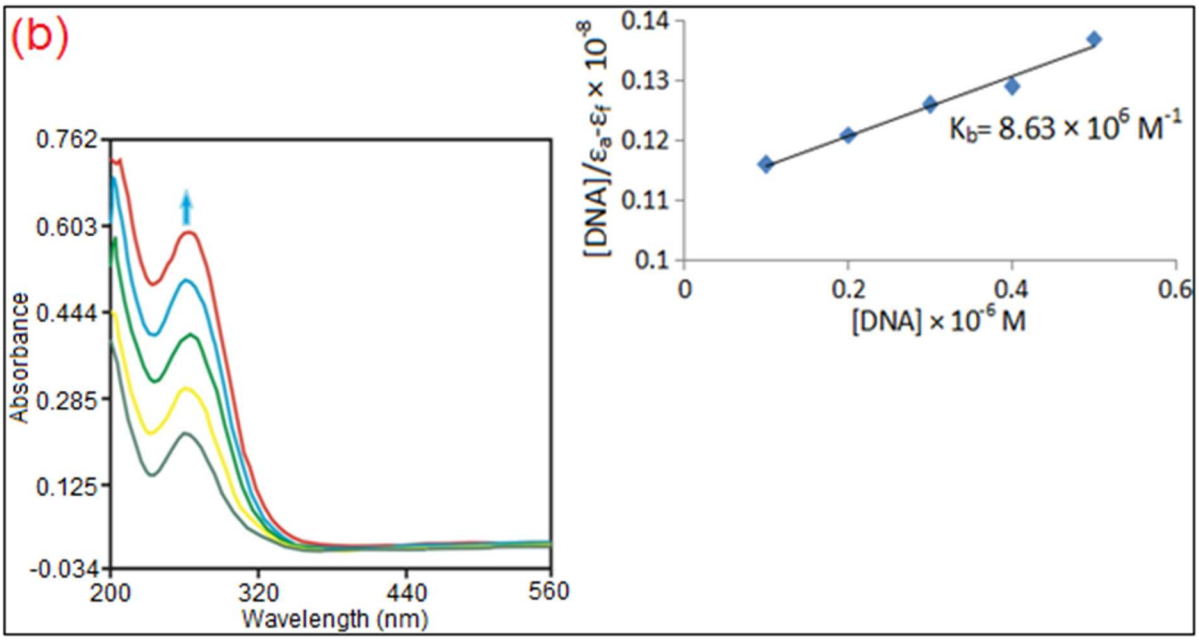

Fig.16.(a), (b). Absorption trace of copper(II) complexes with plot of [DNA]/(ε_a-ε_f) versus [DNA]

Antimicrobial activity

The bacterial activity of newly prepared copper(II) complexes wasexamined by their *zone of inhibition* and *minimum inhibitory concentration* (MIC) on the bacterial species. The complexes were screened for their in *vitro* antimicrobial activity against certain pathogenic bacterial and fungal species at three different concentrations. Compounds**L1, L2, C1,**and**C2** were tested against two-gram positive bacteria such as*Streptococcus pneumoniae* and *Staphylococcus aureus,* three gram-negative bacteria,*Acinetobacter baumannii, Pseudomonas aeruginosa, Klebsiella pneumoniae* and five fungi,*Candida albicans, Candida tropicalis, Trichophyton rubrum, Aspergillus niger and Aspergillus fumigatus* and their MIC (minimum inhibitory concentration) values are provided in Fig. 17 and 18 and Tables8 and 9. The variation in the antimicrobial activity of different metal ligands and copper complexes against different pathogens depends on their impermeability of the cell or the differences in ribosomes in the microbial cell [34]. From the results,it is observed that the complexes exhibited significant activity, but they did not reach the effectiveness of the conventional bactericide *Gentamicin* and fungicide ketoconazole. Tested complexes were shows better activity against all human pathogens, and the results were confirmed by comparing with the standard drug. Among the four compounds, the **C2** exhibited good activity against all five fungi.However, the antimicrobial activity of the newly prepared ligands andcopper(II) complexes were significant when compared with the already reported copper(II) complexes [35, 36].

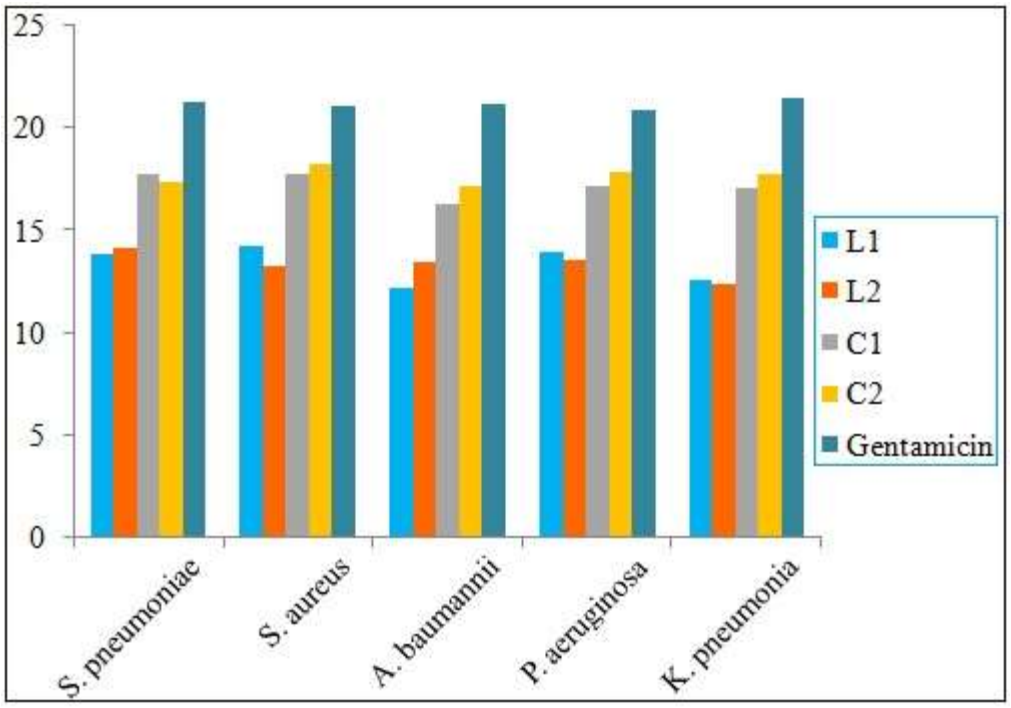

Fig. 17. Antibacterial activity of ligands and copper(II) complexes

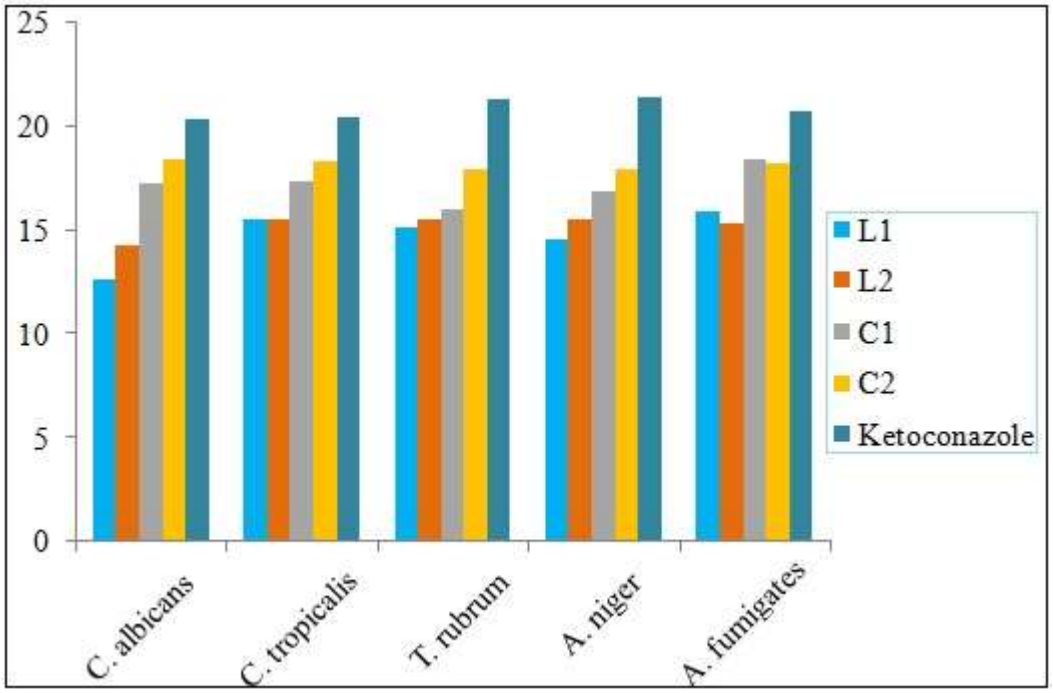

Fig. 18. Antifungal activity of ligands and copper(II) complexes

Antiproliferative studies

Cytotoxicity effects: Carcinoma cell growth inhibition

The results obtained from DNA/Protein binding and antimicrobial studies have shown that the copper(II) complexes and their ligands were studied here have therapeutic potentials and were subjected to anticancer activity. The coumarin derivatives have shown considerable anticancer activity against several cell lines. The in *vitro* antiproliferative activity of the tested ligands **(1** and **2)**

and complexes**(1** and **2)** on the proliferation of human breast cancer cell line MCF-7, human lung cancer cell line A-549 and human cervical cancer cell line HeLa were assayed by the *3-(4, 5-dimethylthiazole-2-ly)-2, 5-diphenyltetrazolium bromide* (MTT) colorimetric assay in a dose-dependent fashion. For comparisons, the cancer activity of *cisplatin* was evaluated under the same experimental condition. *Cisplatin*, a well-known metallodrug currently used in the clinic, was assayed as a positive control. The dose-dependent cell death-inducing ability of the compounds has been analyzed by mean of a graph between the percentages of the cell viability *versus* concentration of the compounds (Fig.19-22) and expressed with IC_{50} values (Fig. 23-25) (Table10, 11).

The anticancer activity of the ligands (1-2) follows the order cisplatin; MCF-7 is 1.16±0.15, A-549 is 1.10±0.10 and HeLa is 1.18±0.12 < **L1** (1.53±0.12), (1.43±0.02) and (1.56±0.08) < **L2** (1.66±0.05), (1.45±0.07) and (1.67±0.08) complexes**(1-2)** follows the order *cisplatin*; MCF-7 is 0.91±0.04, A-549 is 0.87±0.03 and HeLa is 0.95±0.08 < **C2** (1.12±0.48), (1.22±0.48) and (1.16±0.22) < **C1** (1.14±0.67), (1.23±0.22) and (1.18±0.33). The compounds exhibited a high cytotoxic effect on cancer cells with low IC_{50} values indicating their efficiency in killing cancer cells even at low concentrations. The chelation of the ligands with metal ion is responsible for the high cytotoxicity of the complexes. The enhancement in the antitumor activity of the complexes can be related to the electron-donating nature of the N-terminal substitution of the coordinated ligands. Among the copper(II) complexes having the neutral ONO coordinated ligand, it should be noted that high antiproliferative activity was observed in human breast cancer cell line MCF-7, human lung cancer cell line A-549 and human cervical cell lines HeLa.

The results show that the ligands **(1-2)** and copper(II) complexeshave been arranged in the order**L1 < L2**and**C2 < C1**. Interesting bythese results are very similar to that of the DNA binding studies results. To investigate the selectivity of the complexes for the cancer cells rather than the normal cell lines, the ligands and complexes were also screened against human keratinocyte cancer cell lines (HaCaT). The IC_{50} values of the compounds against human normal keratinocyte cancer cells (HaCaT) inferred that the ligands and complexes are non-toxic to normal cells. Moreover, the cytotoxic efficiencies of the presentcopper(II) complexes and their ligands were against these cell lines were found to be higher than the standard positive control,*cisplatin*. The complex **C2** exhibited higher activity than the remaining three compounds. The compounds showed anticancer activity in the order C2>C1>L2>L1, this result pattern is very similar to that of the DNA and protein binding studies results. Moreover, the antiproliferative effects of the new ligands and copper(II) complexes against those cell lines were found to be higher than that of already reported Cu(II) complexes [37-39]

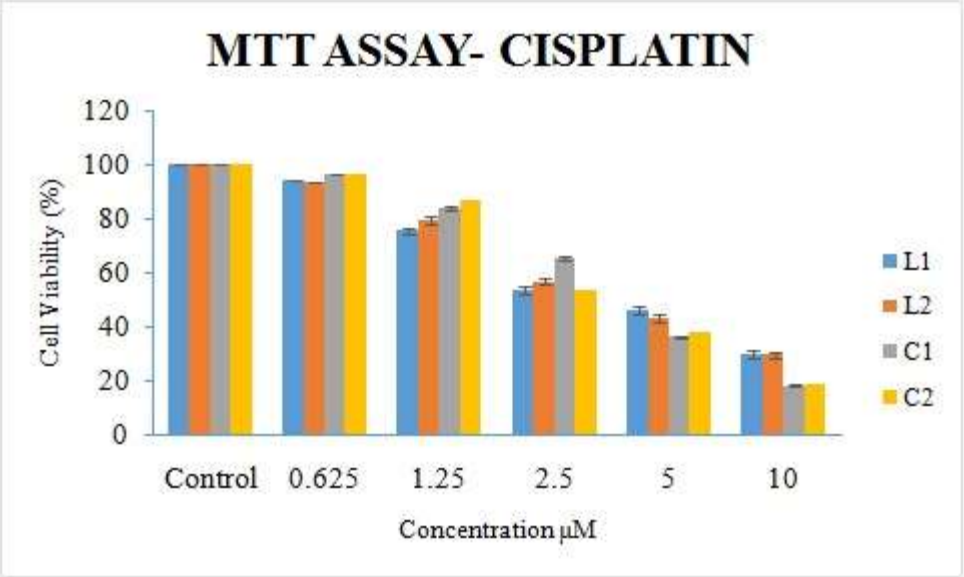

Fig. 19. Human breast cancer cell lines (MCF-7) of ligands and complexes for different concentration

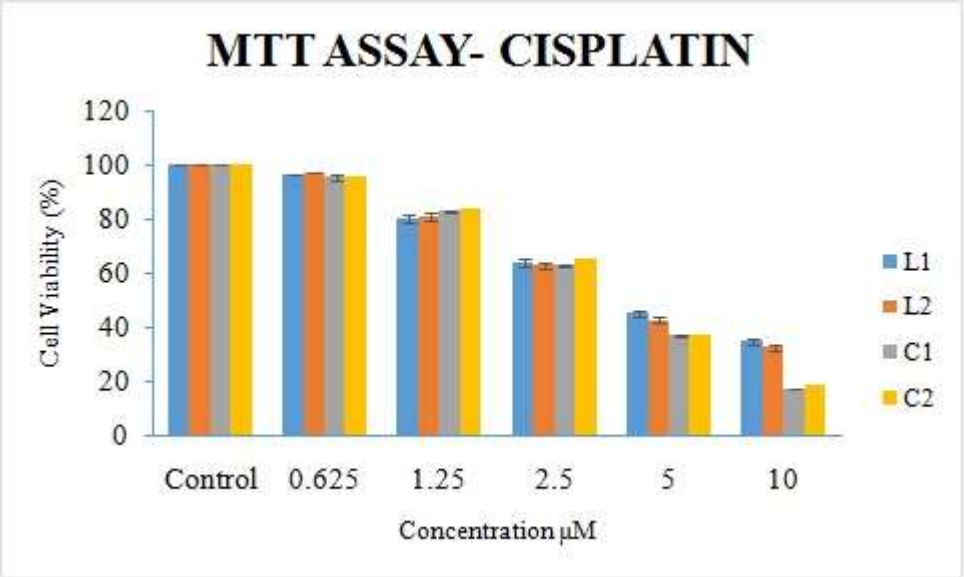

Fig. 20. Human lung cancer cell lines (A-549) of ligands and complexes for different concentration

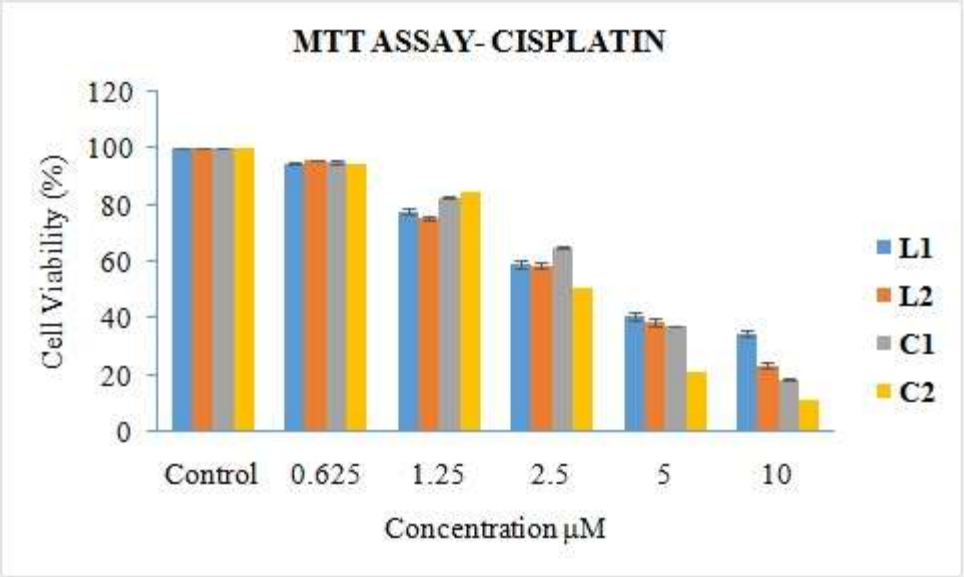

Fig. 21. Human cervical cancer cell lines (HeLa) of ligands and complexes for different concentration

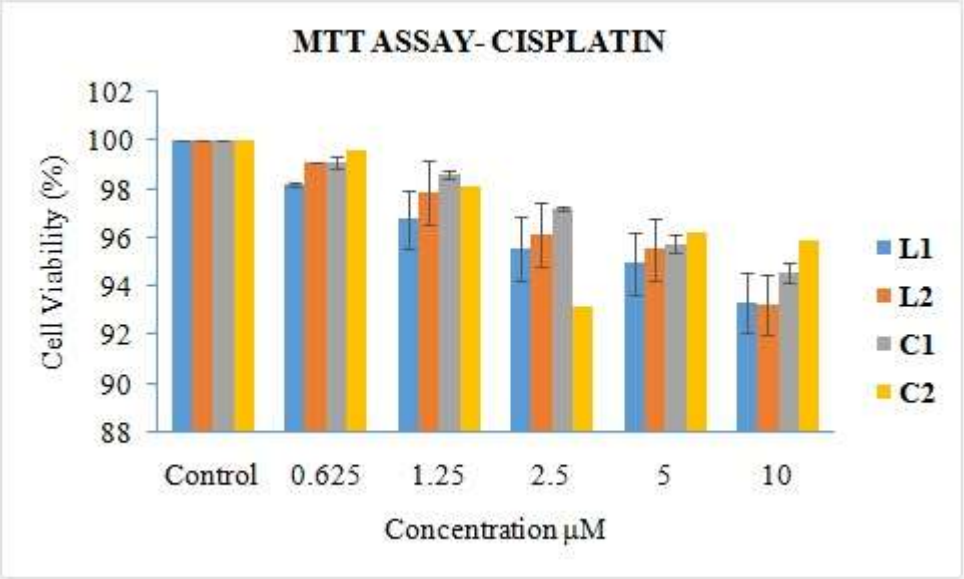

Fig. 22. Human keratinocyte cancer cell lines (HaCaT) of ligands and complexes for different concentration

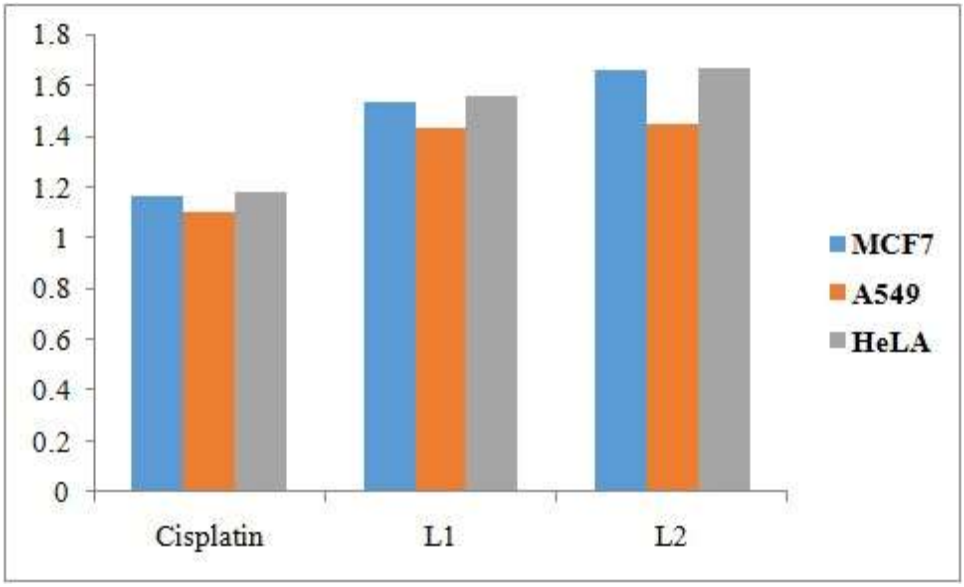

Fig. 23. IC_{50} of ligands

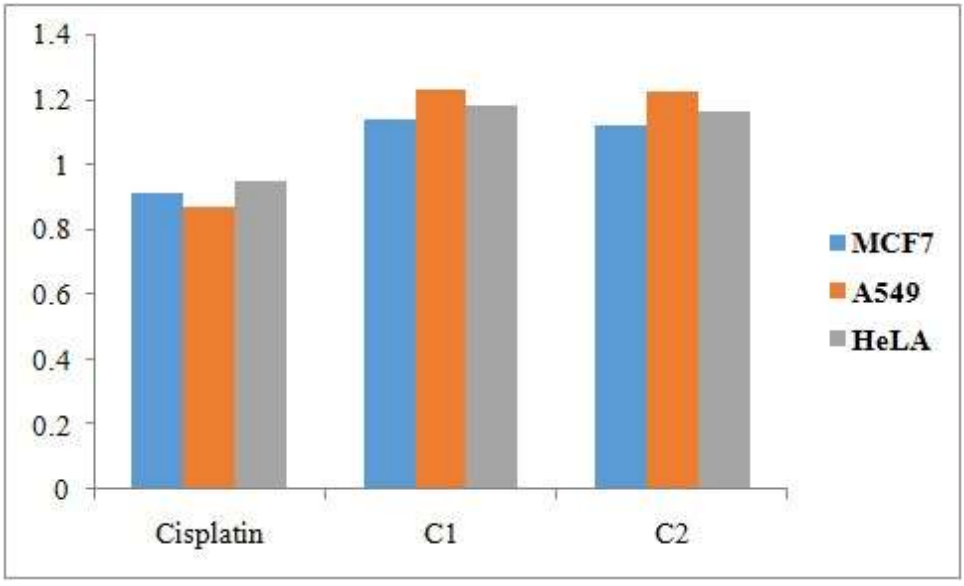

Fig. 24. IC_{50} of copper(II) complexes

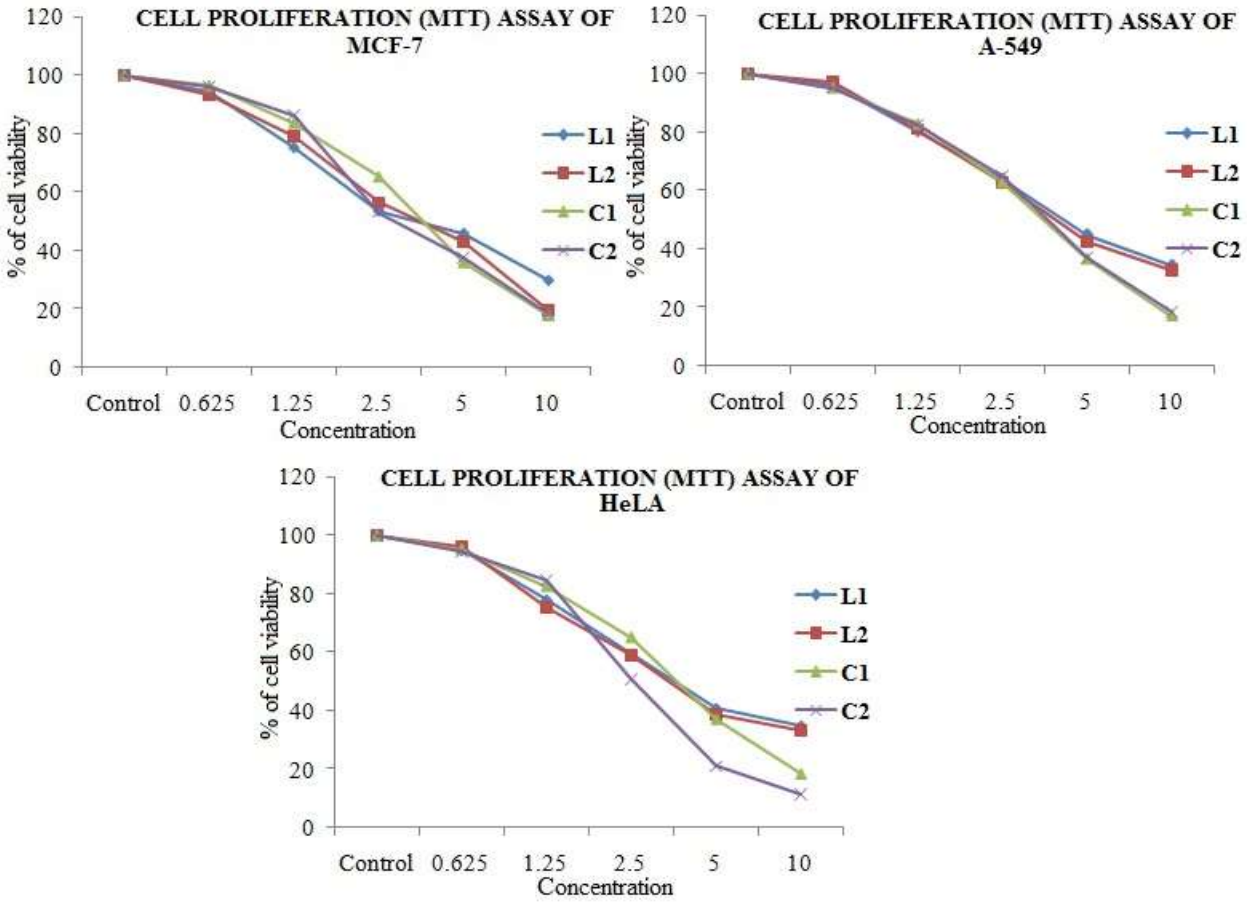

Fig. 25. The newly synthesized ligands (1, 2) and copper(II) complexes (1-2) inhibit MCF-7, A-549, HeLa cells proliferation in a dosed manner. MCF-7, A-549, and HeLa cells were treated with different concentrations of compounds for 48 h, the cell viability was determined and the results were expressed as percentage cell viability with control. Results shown are mean, which are three separate experiments performed in triplicate.

References

1. C. Sonia, B.N. Sivasankar, *Synth. React. Inorg, Metal-Org, Nano-Metal Chem.*, 44, **2014,** 1119-1127.
2. B.N. Sivasankar, *J. Therm. Anal. cal.*, 86, **2006,** 385-392.
3. A.B. Thathan Premkumar, A. Rajendran Selvakumar, P. Nigam, Rathc and Subbiah, S. Govindarajana, *Afr. J. Chem*., 67, **2014**, 85-90.
4. R. Ragul, L. Vikram, B.N. Sivasankar, *Synth. React. Inorg, Metal-Org., and Nano-Metal Chem.*, 45, **2015**, 1069-1079.
5. J.D. Martin-Ramos, *Polyhedron*, 15, **1996**, 439-446.
6. J.D. Martin-Ramos, J.M. Tercero-Moreno, A. Matilla-Hernandez, J. Niclos-Gutierrez, A. Busnot, S. Ferrer. *Polehedron*, 15, **1996**, 439-446.
7. D. Gajapathy, S. Govindarajan, K.C. Patil, H. Manohar, *Polyhedron*,9, **1983,** 865-873.
8. L. Vikram, B.N. Sivasankar, *J. Therm. Anal. Cal.*, 91, **2008,** 963-970.

9. A.I. Vogel, A Text Book of Quantitative Inorganic Analysis (third ed.), Longmans: London, **1962**.
10. Erdey, I. Buzaz, Gravimetric Analysis (Part II), *Pergamon*, London **1965.**
11. A.I. Vogel, A Text Book of Quantitative Inorganic Analysis (second ed.), Longmans, London, **1951**.
12. K. Johnson, ORTEP ORNL-3794, Oak Ridge National Laboratory, Tennessee, **1976**.
13. G.M. Sheldrick, SHELXL-97 programs for crystal structure determination, University of Cambridge, England, **1977**.
14. J. Marmur, *J. Mol. Biol*., 3, **1961**, 208-218.
15. C.V. Kumar, E.H. Asuncion, *J. Am. Chem. Soc*., 115, **1993,** 8547-8553.
16. P.R. Reddy, K.S. Rao, B. Satyanarayana, *Tetrahedron Lett*.,47, **2006,** 7311-7315**.**
17. I. Wiegand, K. Hilpert, R. Hancock, *Nat. Protocol.,* 3, 2008, 163.
18. T. Mossman, *J. Immunol. Methods,* 65, 1983, 55.
19. H.J. Motulsky, Prism 5 Statistics Guide, Graph Pad Software Inc., San Diego, CA, 2007, http://www.graphpad.com.
20. S. Roy, P. Mitra, A.K. Patra, *Inorg. Chem. Acta.,* 370, **2011**, 247-253.
21. R. Selvakumar, S.J. Geib, A.M. Sankar, T. Premkumar, S. Govindharajan, *J. Phy. Chem. Solids,* 86, **2015**, 49-56.
22. B.N. Sivasankar, S. Govindharajan, *Ind. J. Chem.,* 3, **1994**, 329-311.
23. A. Braibanti, F. Dallavalle, M.A. Pellingghalli, E. Laperati, *Inorg. Chem.,* 7, **1968**, 1430.
24. B.N. Sivasankar, S. Govindharajan, *Mater. Res. Bull.,* 31, **1996**, 47-54.
25. L. Ragunath, B.N. Sivasankar, *J. Chem. Crystallogr.,* 40, **2010**, 1170-1174.
26. R. Ragul, B.N. Sivasankar, *J. Chem. Crystallogr.,* 42, **2012**, 533-542.
27. R. Pradeep, K. Naresh, T.M. Ahamed Hussain, L. Vikram, B.N. Sivasankar, *J. Saudi. Chem. Soc.,* 21, **2017**, 358-365.
28. L. Vikram, B.N. Sivasankar, *J. Therm. Anal. Cal.,* 91, **2008**, 963-970.
29. E.K. Efthimiadou, A. Karalioto, G. Psomas, *J. Inorg. Biochem.,* 104, **2010**, 455.
30. E.C. Long, J.K. Barton, *Acc. Chem. Res.,* 23, **1990**, 271.
31. M. Muralisankar, J. Haribabu, N.S.P. Bhuvanesh, R. Karvembu, A. Sreekanth, *Inorg. Chim. Acta.,* 449, **2016**, 82.
32. S. Chandra, S. Verma, *Russ. J. Coord. Chem.,* 34, **2008**, 449.
33. L. Andrezalov, J. Plsikova, J. Janockova, K. Konarikova, I. Zitnanova, M. Kohutova, M. Kozurkova, *J. Organomet. Chem.,* 827, **2017**, 67.
34. P.G. Lawrence, P.L. Harold, O.G. Francis, *Antibiot. Chemother.,* 4, **1957**, 1980.
35. P. Kavitha, M. Saritha, K. Laxma Reddy, B. Naresh Kumar, Ch. Apparao, K. Seshaiah, *Spectrochim. Acta A.,* 101, **2013**, 164.
36. M. Muralisankar, S. Sujith, N.S.P. Bhuvanesh, A. Sreekanth, *Polyhedron*, 118, **2016**, 103.
37. M. Anjomshosa, M. Torkzadeh-Mahani, Spectrochimica Acta Part A: *Molecul. Biomolecul. Spectros.,* 150, **2015**, 390.
38. Y. Gou, J. Li, B. Fan, B. Xu, M. Zhou, F. Yang, *Eur. J. Med. Chem.,* 134, **2017**, 207.

SUPPLEMENTARY RESULTS

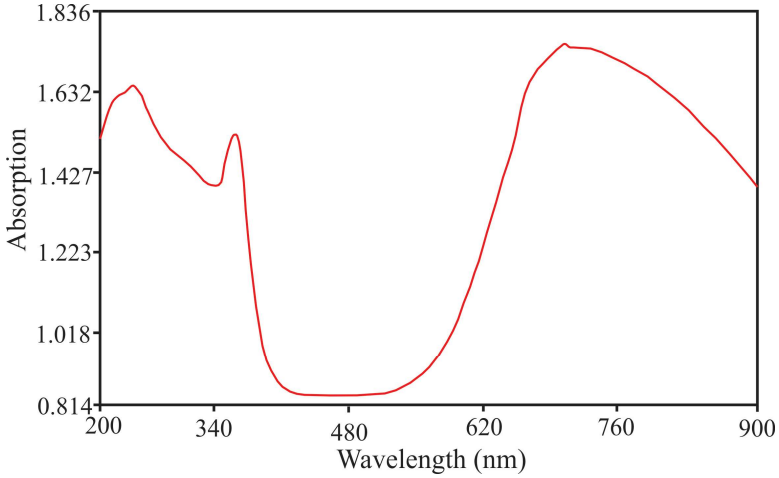

SF. 1. Electronic spectrum of (HAgun)[Cu(edta)].3H_2O

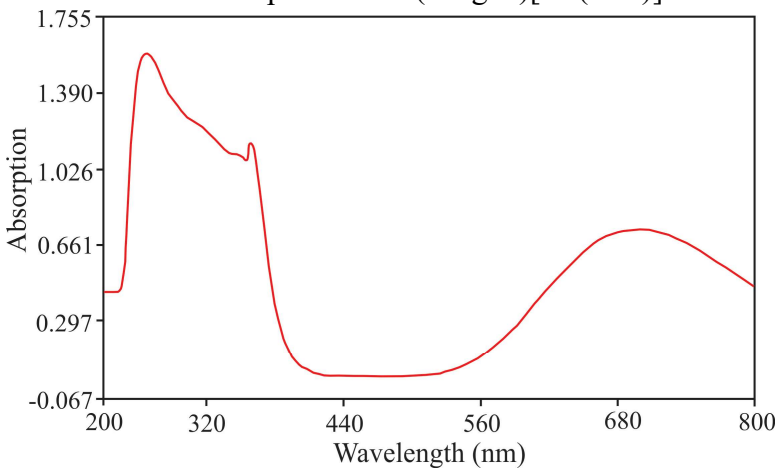

SF. 2. Electronic spectrum of (HAgun)[Cu(Hcdta)].H_2O

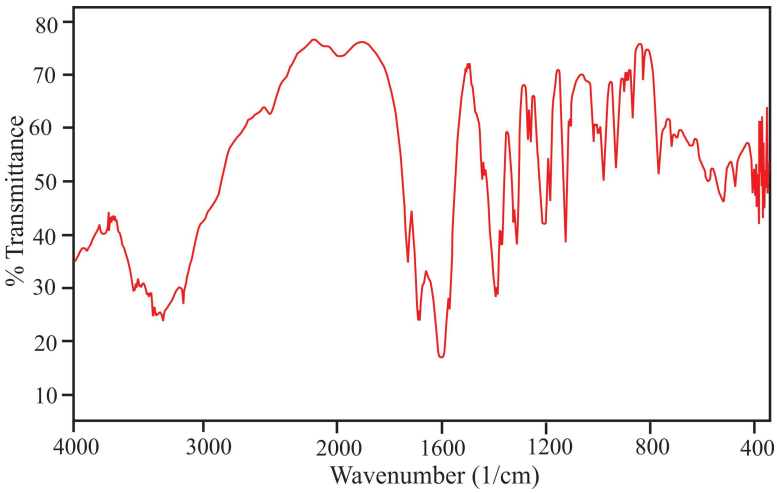

SF. 3. IR spectrum of (HAgun)[Cu(Hedta)].3H_2O

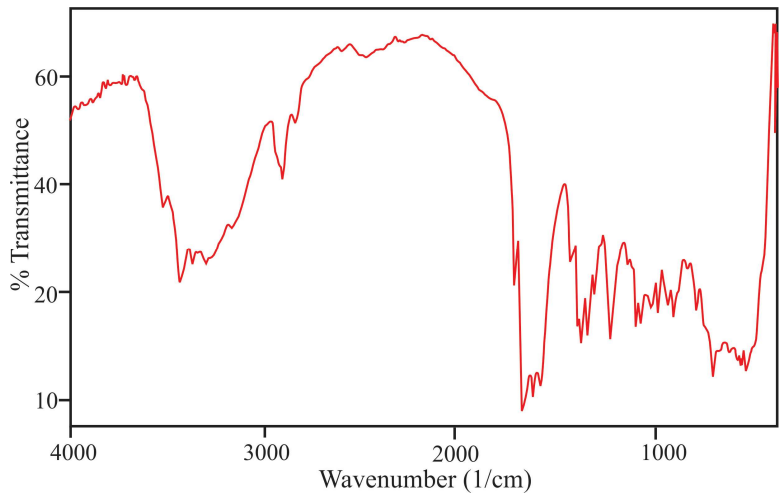

SF. 4. IR spectrum of (HAgun)[Cu(Hcdta)].H_2O

ST. 1. Thermal data of salts and complexes

Compound	DTA peak Temp. (°C)	TG temp. Range (°C)	TG weight loss (%) Found	TG weight loss (%) Calc.	Residue
$(HAgun)_2(H_2edta).3H_2O$	95 (+)	73-110	11.20	10.90	$(HAgun)_2(H_2edta)$
	400 (+)	98-580	99.40	100.00	-
$(HAgun)_2(H_2cdta).H_2O$	90 (+)	80-100	4.10	3.52	$(HAgun)_2(H_2cdta)$
	370 (+)	100-580	98.90	100.00	-
$(HAgun)[Cu(Hedta)].3H_2O$	92(+)	75-150	12.30	11.20	(HAgun)[Cu(Hedta)]
	227(+)	150-250	28.60	27.00	$[Cu(H_2edta)]$
	372(+)	250-380	38.00	37.50	$Cu(CH_3COO)_2$
	450(+)	380-520	75.00	74.00	$CuCO_3$
$(HAgun)[Cu(Hcdta)].H_2O$	180(+)	90-210	4.50	3.60	(HAgun)[Cu(Hcdta)]
	240(+)	210-280	17.50	18.60	$[Cu(H_2cdta)]$
	291(+)	280-330	37.30	36.00	$Cu(CH_3COO)_2$
	380(+)	330-580	75.18	75.30	$CuCO_3$

ST. 2. Antibacterial activity of new salts **(1 and 2)** and Cu(II) Complexes **(1** and **2)**

Compounds	**Concentration**	**Zone of inhibition (mm) against bacteria**				
	(µg/ml)	***S. pneumoniae***	***S. aureus***	***A. baumannii***	***P. aeruginosa***	***K. pneumonia***
L1	25	-	-	-	-	-
	50	9.58±0.11	8.95±0.12	8.45±0.14	9.58±0.45	9.78±0.44
	100	13.85±0.68	14.25±0.27	12.11±0.37	13.89±0.79	12.57±0.29
L2	25	-	-	-	-	-
	50	9.12±0.23	7.56±0.34	10.71±0.51	9.45±0.25	9.22±0.29

	100	14.10±0.08	13.25±0.55	13.40±0.26	13.56±0.47	12.36±0.17
C1	25	-	-	-	-	-
	50	13.11±0.11	14.50±0.05	13.53±0.31	14.91±0.91	15.16±0.31
	100	17.71±0.33	17.78±0.62	16.31±0.12	17.19±0.41	17.10±0.23
C2	25	-	-	-	-	-
	50	13.98±0.51	15.60±0.32	16.59±0.81	15.18±0.01	15.61±0.13
	100	17.31±0.21	18.26±0.13	17.13±0.21	17.87±0.12	17.78±0.62
Gentamicin	25	21.26±0.55	21.09±0.58	21.22±0.54	20.87±0.59	21.49±0.65

ST. 3. Antifungal activity of new salts **(1 and 2)** and Cu(II) Complexes **(1 and 2)**

Compounds	**Concentration**	**Zone of inhibition (mm) against bacteria**				
	(µg/ml)	***C. albicans***	***C. tropicalis***	***T. rubrum***	***A. niger***	***A. fumigates***
L1	25	-	-	-	-	-
	50	7.35±0.77	11.25±0.92	12.66±0.52	10.53±0.15	12.10±0.16
	100	12.65±0.14	15.50±0.48	15.11±0.22	14.57±0.66	15.89±0.76
L2	25	-	-	-	-	-
	50	8.66±0.36	10.28±0.13	13.65±0.44	11.85±0.43	11.56±0.33
	100	14.25±0.58	15.56±0.96	15.54±0.56	15.55±0.87	15.32±0.97
C-3	25	-	-	-	-	-
	50	12.32±0.48	14.46±0.36	13.30±0.45	14.25±0.52	17.51±0.22
	100	17.32±0.48	17.35±0.31	16.04±0.05	16.91±0.22	18.41±0.21
C-4	25	-	-	-	-	-
	50	16.41±0.96	14.65±0.16	15.32±0.61	15.50±0.26	16.94±0.51
	100	18.41±0.96	18.35±0.35	17.95±0.66	17.91±0.23	18.26±0.13
Ketoconazole	25	20.39±0.29	20.48±0.43	21.34±0.11	21.39±0.32	20.78±0.45

ST. 4. The IC50 values for the human breast cancer cell line MCF-7, human lung carcinoma cancer cell line A549, human cervical cancer cell line HeLa and human normal keratinocyte cells (HaCaT) with the ligands (**1-6**) for 48h.

Compound	**IC50 values (µM)**			
	MCF7	**A549**	**HeLa**	**HaCaT**
Cisplatin	1.16±0.15	1.10±0.10	1.18±0.12	>90
L-3	1.53±0.12	1.43±0.02	1.56±0.08	>90
L-4	1.66±0.05	1.45±0.07	1.67±0.08	>90

ST. 5. The IC50 values for the human breast cancer cell line MCF-7, human lung carcinoma cancer cell line A549, human cervical cancer cell line HeLa and human normal keratinocyte cells (HaCaT)

with the copper(II) complexes (**1-6**) for 48h.

Compound	IC50 values (μM)			
	MCF7	**A549**	**HeLa**	**HaCaT**
Cisplatin	0.91±0.05	0.87±0.03	0.95±0.04	>90
C-3	1.14±0.67	1.23±0.22	1.18±0.33	>90
C-4	1.12±0.48	1.22±0.48	1.16±0.22	>90